ISSN 0031-918X, Physics of Metals and Metallography, 2023, Vol. 124, No. 2, pp. 126–132. © The Author(s), 2023. This article is an open access publication, corrected publication 2023.
Russian Text © The Author(s), 2023, published in Fizika Metallov i Metallovedenie, 2023, Vol. 124, No. 2, pp. 134–140.

ELECTRICAL AND MAGNETIC PROPERTIES

Magneto-Optical Spectroscopy of Nanocomposites $(CoFeB)_x(LiNbO_3)_{100-x}$ with Concentrations up to the Percolation Threshold: From Superparamagnetism and Superferromagnetism to Ferromagnetism

E. A. Gan'shina[a, *], I. M. Pripechenkov[a], N. N. Perova[a], E. S. Kanazakova[a], S. N. Nikolaev[b], A. S. Sitnikov[b, c], A. B. Granovskii[a, d], and V. V. Ryl'kov[b, d]

[a] *Department of Physics, Moscow State University, Moscow, 119991 Russia*
[b] *National Research Center Kurchatov Institute, Moscow, 123182 Russia*
[c] *Voronezh State Technical University, Voronezh, 394026 Russia*
[d] *Institute of Theoretical and Applied Electrodynamics, Russian Academy of Sciences, Moscow, 125412 Russia*
**e-mail: eagan@mail.ru*

Received September 21, 2022; revised December 2, 2022; accepted December 5, 2022

Abstract—Nanocomposites $(CoFeB)_x(LiNbO_3)_{100-x}$ with $x = 17–48$ at % have been synthesized by ion beam sputtering of a composite target comprised of $Co_{40}Fe_{40}B_{20}$ and $LiNbO_3$ onto silicon substrates, and the transitions from the superparamagnetic state to the superferromagnetic and ferromagnetic states with an increase in the concentration of the magnetic component are studied by magneto-optical methods. The magneto-optical properties have been investigated in the geometry of the equatorial (transverse) Kerr effect (TKE). Magneto-optical spectra are recorded in the range of 0.5–4.0 eV in fields up to 2.5 kOe at 20–300 K, field and temperature dependences of the TKE at certain wavelengths are obtained, and the domain structure during magnetization reversal is visualized using a magneto-optical Kerr microscope. It is shown that the sample with $x = 17$ at % is superparamagnetic at temperatures above the blocking temperature (about 30 K). The interaction between the granules is considerable already at $x = 20$ at %, the transition to the superferromagnetic state occurs at $x \approx 32–36$ at %, and the transition to the ferromagnetic state occurs at $x \approx 44$ at % near the metal–dielectric transition, i.e., at a concentration below the percolation transport threshold.

Keywords: nanocomposites, magneto-optics, superparamagnetism, superferromagnetism
DOI: 10.1134/S0031918X22601949

INTRODUCTION

Magnetic nanocomposites or ferromagnetic metal–dielectric nanogranular magnetic films are ensembles of single domain ferromagnetic metal particles in a dielectric matrix. Depending on the metal content (and especially near the percolation threshold), they exhibit interesting magnetic, magnetotransport, optical, magneto-optical, and high frequency properties. Magnetic nanocomposites are widely used in engineering, for example, as materials for magnetic recording of information or high frequency reflective coatings. They are also promising for applications in information recording and storage systems, magnetic sensors, optoelectronic materials, etc. [1]. It has recently been shown that magnetic nanocomposites also show the effect of reversible resistive switching, which is promising for the creation of memristor devices that mimic synapses in neuromorphic systems [2]. The memristive effect is most pronounced in $(CoFeB)_x(LiNbO_3)_{100-x}$ nanocomposites with metal concentrations up to the percolation threshold. Due to the high sensitivity of magneto-optical techniques, magnetic nanocomposites can be considered as an optimal platform for studying various properties of disordered systems by magneto-optical methods.

With low concentrations of magnetic nanoparticles (much lower than the percolation threshold x_{per}), they slightly interact with each other via dipole–dipole interactions or exchange coupling, so the nanocomposite is an ensemble of single domain particles at temperatures below blocking temperature T_b and an ensemble of superparamagnetic particles at $T_b < T < T_C$, where T_C is the Curie temperature of an individual particle. With an increase in the concentration x, the interaction between magnetic particles at $T < T_{sf}$ (where T_{sf} is determined by the coupling intensity) leads to a superferromagnetic state [3], which at higher temperatures $T_{sf} < T < T_{sp}$ is replaced by a superparamagnetic behavior. In the ideal case, superferromagnetism is characteristic of an ensemble in which the magnetic moments of all nanoparticles are predominantly oriented in the same direction. In the nonideal

case, the system consists of superferromagnetic regions and superparamagnetic particles. Finally, a transition to the ferromagnetic state occurs with a further increase in the concentration to x_{ferro}. The ferromagnetic percolation threshold x_{ferro} by no means coincides with transport percolation threshold x_{per}. The composite with $x > x_{per}$ is a metal, but the transition to a dielectric state with hopping conductivity occurs at $x = x_{MI}$, and the composite is characterized by a tunnel type of conductivity in the concentration range of $x_{MI} < x < x_{per}$ [4]. It should also be noted that the presence of magnetic ions in intergranular gaps has a substantial effect on the values of critical parameters x_{ferro}, x_{MI}, and x_{per}, which complicates possible scenarios of magnetic behavior [1].

In this study, magneto-optical spectroscopy (MOS) is used to analyze the magnetic properties of $(CoFeB)_x(LiNbO_3)_{100-x}$ nanocomposites containing a metallic phase below the transport percolation threshold. In [1, 2, 5–9], the structural, magnetic, and transport properties of $(CoFeB)_x(LiNbO_3)_{100-x}$ nanocomposites synthesized under different technological conditions and on different substrates were studied to optimize the memristive properties. Magneto-optical techniques have not been used before for studying the magnetic properties of these nanocomposites, including studying the transitions from superparamagnetic behavior to superferromagnetism and ferromagnetism. This study was aimed at investigating the features of the magnetic properties of nanocomposites by magneto-optical spectroscopy.

EXPERIMENTAL

Samples of nanogranular films $(CoFeB)_x(LiNbO_3)_{100-x}$ with x = 17–48 at % were obtained by sputtering a composite target comprised of $Co_{40}Fe_{40}B_{20}$ and $LiNbO_3$ by an ion beam onto silicon substrates. The film thickness was 0.16 μm. The details of sample preparation and their structural characterization are similar to those described earlier [1, 2].

Electron microscopy studies with a nanometer resolution, which were performed using a TITAN 80–300 scanning (TEM/STEM) electron microscope (FEI, U.S.A.), showed that the obtained nanocomposite films consist of metallic granules in an amorphous nonstoichiometric $LiNbO_y$ matrix. Moreover, the granules have a size of $d \approx 2$–5 nm and a shape close to spherical with slight elongation along the growth direction.

Electrical resistance measurements showed that the temperature dependence of conductivity is described by a logarithmic law characteristic of strong tunneling coupling for the sample with $x = 48$ at % and by a law characteristic of hopping conductivity for the sample with $x = 42$ at %. This means that the percolation transport threshold is $x_{per} \geq 48$ at %, and the compositions of all studied samples have x values that are below the transport percolation threshold, while the metal–dielectric transition occurs in the vicinity of $x = 42$–44 at %.

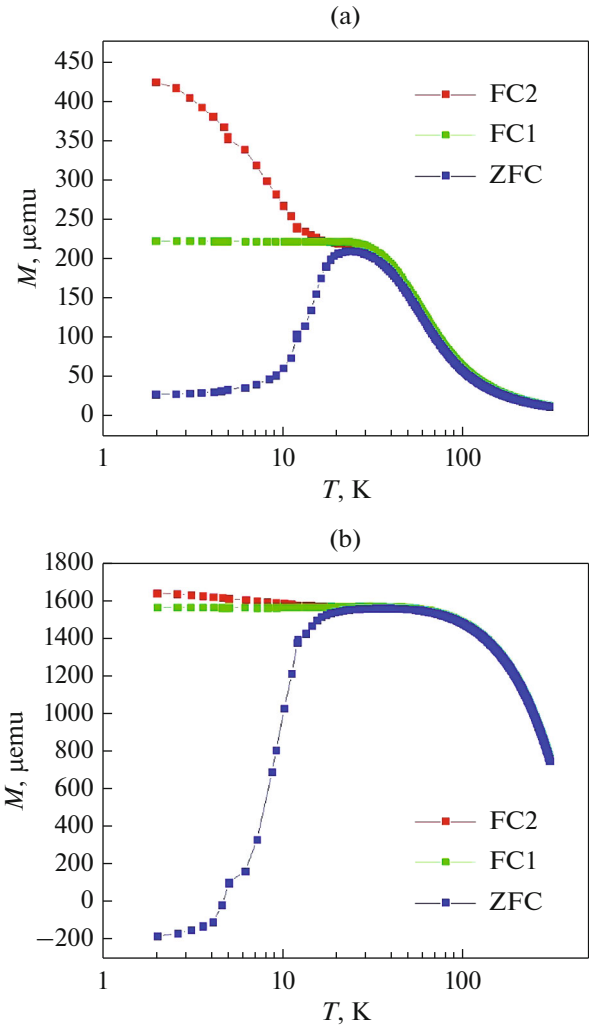

Fig. 1. The temperature dependences of the magnetic moment of structures with (a) $x = 17$ at % and (b) $x = 42$ at % measured during their heating in a field of 100 Oe after cooling in a zero field (ZFC) and in fields of 100 Oe (FC1) and 10 kOe (FC2).

Magnetic measurements were performed using a QuantumDesign MPMS-XL7 SQUID magnetometer. The measurements were carried out at temperatures of 1.9–350 K in fields oriented in the plane of the samples. Temperature dependences $M(T)$ of the magnetic moments of the structures were studied upon heating in a field of 100 Oe, which were preliminarily cooled under various conditions—namely, in the absence of a field (ZFC), in a field 100 Oe (FC1), and in a field of 10 kOe (FC2).

Figure 1 shows the $M(T)$ temperature dependences for samples with metal contents of $x = 17$ at % and $x = 42$ at %. As can be seen from Fig. 1, the magnetization in both samples below temperatures of around 30–

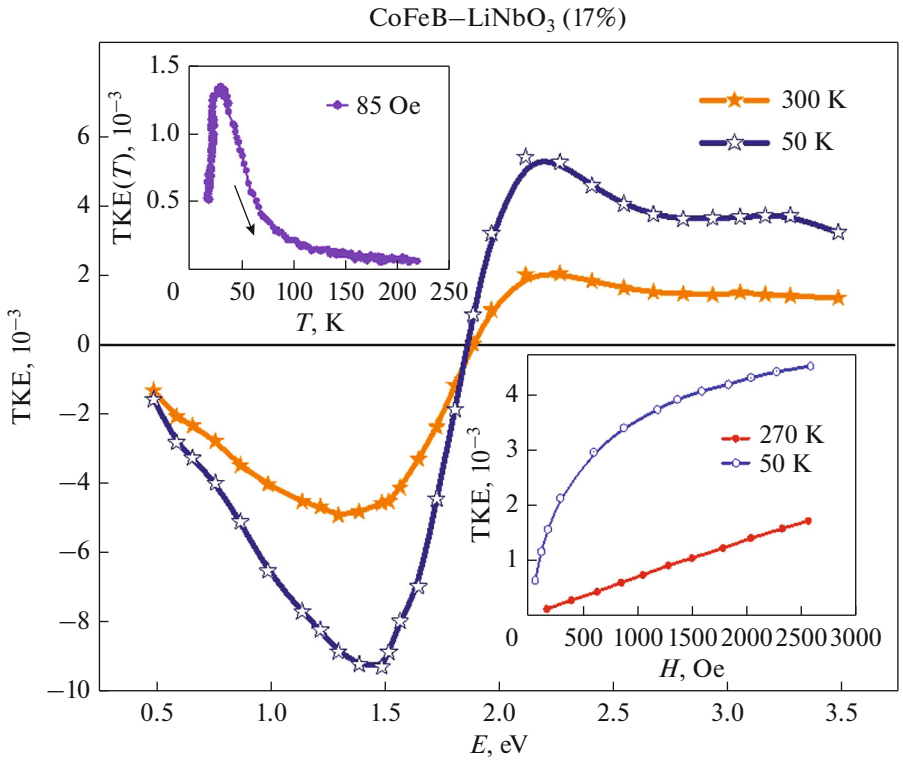

Fig. 2. The spectral dependences of the TKE at two temperatures for a nanocomposite with $x = 17$ at %. The insets show the temperature and field dependences of the TKE.

40 K turns out to be much higher in the case of cooling in a magnetic field, i.e., the blocking temperature at $x = 17$ at % is around 30–40 K.

The MOS studies were carried out in the geometry of the equatorial (or transverse) Kerr effect (TKE) at $T = 20$–300 K in the spectral range 0.5–3.8 eV in a magnetic field of up to 2.5 kOe. We used *p*-polarized light at an angle of incidence of 69.5°. For each concentration, the spectral dependence was measured in the maximum magnetic field. The temperature and field dependences of the MOS signal were measured for a number of selected wavelengths. The measurements were performed by the dynamic method, in which the TKE parameter corresponds to a relative change in the intensity of the reflected light when the sample is magnetized by an alternating-current magnetic field with a frequency of 40 Hz. Moreover, we visualized the domain structure of the samples during magnetization reversal and determined the hysteresis loops of the near-surface region by a Kerr magneto-optic microscope from Evicomagnetics GmbH (Germany) [10]. The measurements were performed at room temperature in the high resolution mode (spot region about 500 μm). The images were processed in the KerrLab software package provided by the device manufacturer.

RESULTS AND DISCUSSION

The field dependence of the MOS signal for a sample with $x = 17$ at % tends to saturation in a strong field at low temperatures and is strictly linear at room temperature (Fig. 2).

The temperature dependence above 40 K is described by the 1/T law. This means that this sample is superparamagnetic at $T < T_b \approx 30$–40 K. This value of the blocking temperature is in good agreement with the data of magnetic measurements (Fig. 1). It should be noted here that the MOS signal on reflection is formed at a depth of $\lambda/4\pi k$, where λ is the radiation wavelength and k is the imaginary part of the refractive index of the composite (attenuation coefficient) [11]. This depth is around 15–20 nm and is obviously less than the film thickness. Hence, the T_b values determined by MOS may differ from the T_b values determined by magnetic methods, which characterize the value averaged over the entire thickness. According to the X-ray diffraction structural data [9], a columnar structure is formed near the substrate in $(CoFeB)_x(LiNbO_3)_{100-x}$ films deposited on glass ceramic substrates, which is replaced by formed spherical granules upon approaching the surface. The practical coincidence of the T_b values determined by MO and magnetic methods indicates that the height of the columnar structure in the studied samples obtained on

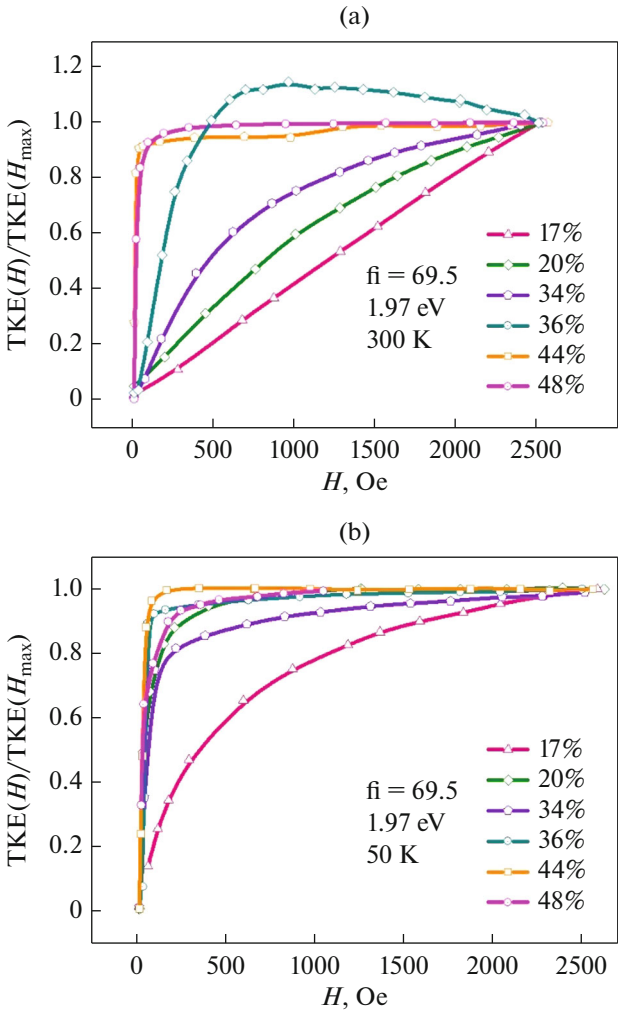

Fig. 3. The normalized field dependences $TKE(H)/TKE(H_{max})$ of $(CoFeB)_x(LiNbO_3)_{100-x}$ nanocomposites at (a) room temperature and (b) a lower temperature of 50 K.

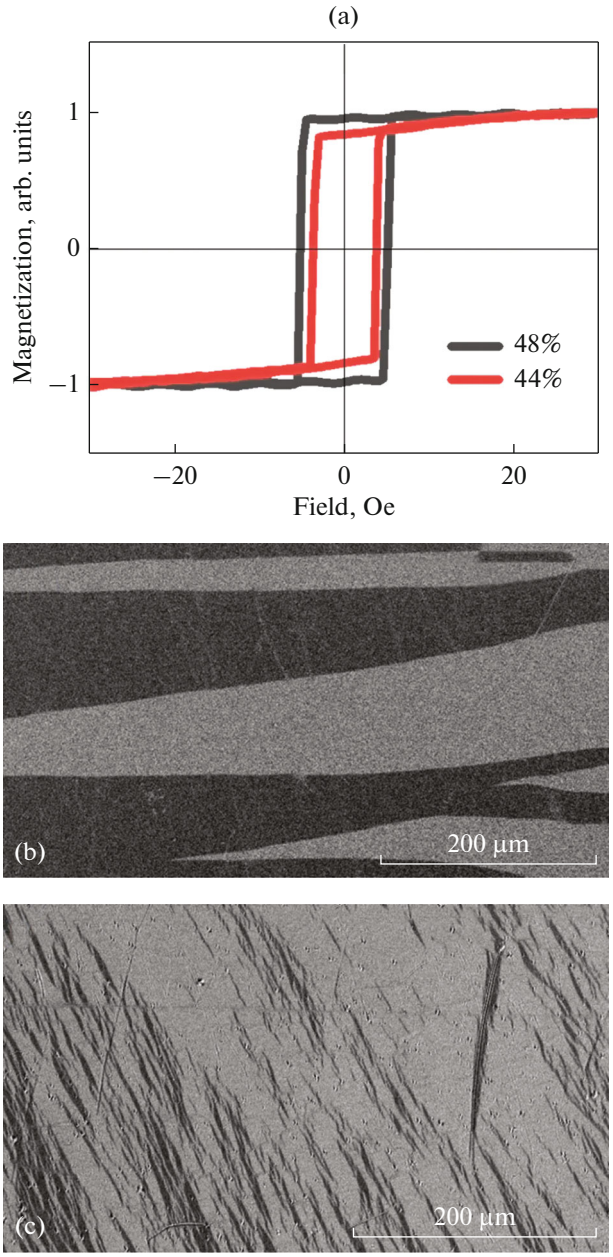

Fig. 4. (a) the normalized hysteresis loops for nanocomposites with $x = 44$ at %, and images obtained on a magneto-optical microscope for the (b) easy axis and (c) hard axis domain structures.

silicon substrates is insignificant compared to the film thickness and there are no substantial variations of the magnetic anisotropy constant over the film thickness.

The field dependences of the MOS signal at a photon energy of 1.97 eV are shown in Fig. 3. The choice of this photon energy was made in such a way so to more clearly show the revealed features of the MOS properties in the superferromagnetic state.

Already at $x = 20$ at %, the TKE signal becomes nonlinear with respect to the field (Fig. 3a). This clearly shows the occurrence of interaction between the granules. With an increase of x, the field dependence of the TKE becomes increasingly nonlinear and similar to that for a ferromagnet.

For compositions with $x = 48$ and 44 at %, the domain structure is visualized using a Kerr magnetometer and hysteresis loops are recorded taking into account changes in the contrast during magnetization reversal (Fig. 4). With $x = 36$ at %, we were unable to visualize the domain structure. Thus, the ferromagnetic percolation threshold is in the vicinity of $x \approx 44$ at %, which is less than the transport percolation threshold and is close to the metal–dielectric transition. That is, long-range ferromagnetic order already appears when a percolation conductivity cluster has not yet formed in the sample and there are tunneling gaps between ferromagnetic particles. The exchange interaction between the granules is accomplished through thin dielectric layers.

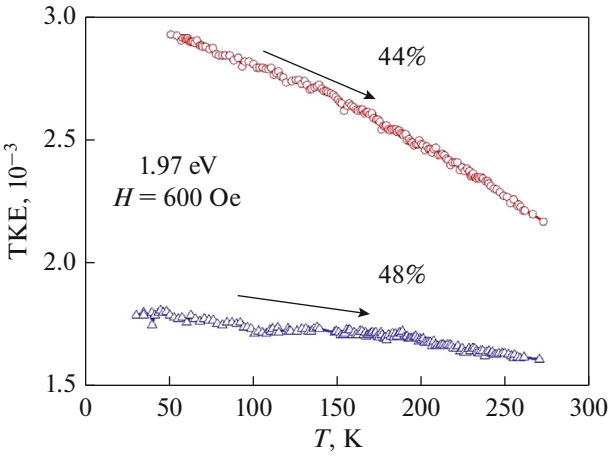

Fig. 5. The temperature dependences TKE(T) of $(CoFeB)_x(LiNbO_3)_{100-x}$ nanocomposites.

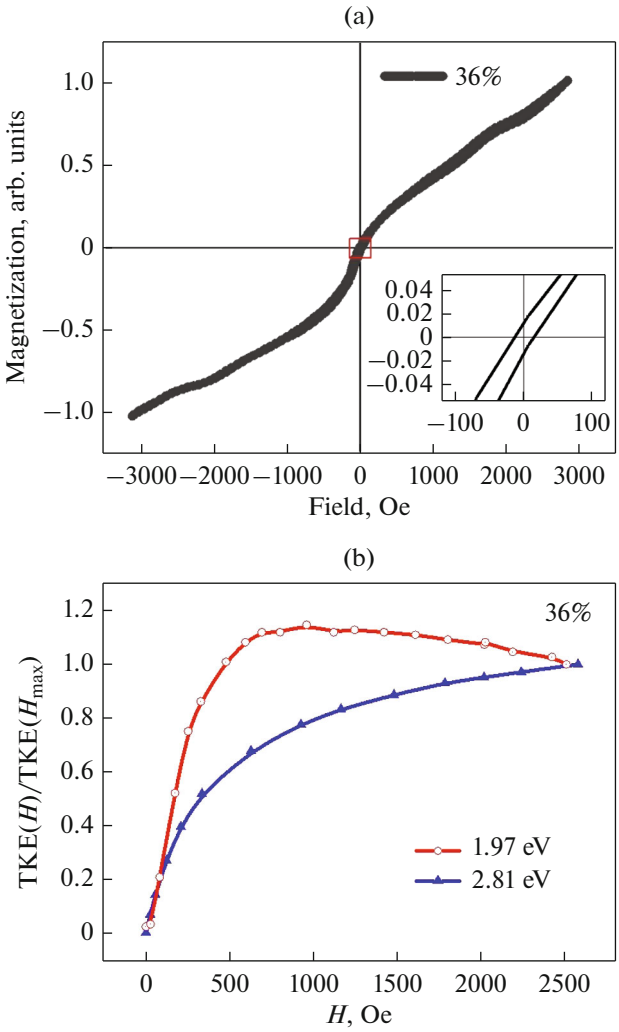

Fig. 6. (a) A hysteresis loop obtained with a MO microscope, and (b) normalized field dependences TKE(H)/TKE(H_{max}) of $(CoFeB)_x(LiNbO_3)_{100-x}$ nanocomposites with x = 36 at %.

The following two features of the magnetic behavior of the sample with $x = 44$ at % should be noted: the sample is easily magnetized and undergoes magnetization reversal in weak magnetic fields, thereby demonstrating magnetic softness; however, the temperature dependence of the MOS signal is not typical of the magnetization of a ferromagnet with a high Curie temperature corresponding to that of CoFeB (Fig. 5). Possible reasons for this behavior are as follows. First, the composition of the granules is not identical to the composition of the target in the ion-beam sputtering process. Secondly, the Curie temperature of nanoparticles can substantially differ from the Curie temperature of the bulk material. Third, the Curie temperature for a sample near the ferromagnetic percolation threshold is determined by the exchange interaction strength between granules, which is lower in the mode of tunneling, rather than by exchange interaction inside the granules. We believe that it is the latter mechanism that plays the main role and the first two mechanisms cannot substantially change the Curie temperature.

The domain structure and coercive force are characteristic of both the ferromagnetic and superferromagnetic states [3], which makes it difficult to find a strictly specified transition threshold between these states. As for the sample with x = 36 at %, it can be stated that it is in an intermediate state when macroscopic regions with a predominant orientation of the magnetic moments of nanoparticles (superferromagnetic regions) coexist with isolated superparamagnetic particles.

This follows not only from the shape of the hysteresis loop (Fig. 6a), but also from the anomalous field dependence of the MOS signal. With a light quantum particle energy of 1.97 eV, the signal first increases with an increase in the field and then begins to decrease in strong fields, while the magnetization increases. For other wavelengths (for example, corresponding to 2.81 eV), the TKE increases with an increase in the field in the same way as the magnetization does (Fig. 6).

This means that there are two fractions in the sample with different magnetic properties. The competition of contributions to the MO signal, namely, the response from superferromagnetic macroscopic regions and superparamagnetic particles, leads to the appearance of an anomalous field dependence of TKE in the spectral region, in which these contributions have different signs [12]. Thus, MO methods make it possible to determine the presence of a superferromagnetic state.

Magneto-optical spectra of nanocomposites are shown in Fig. 7. It is upon the transition from the superparamagnetic behavior (x = 17–20 at %) to the superferromagnetic one that the positions of the characteristic peaks substantially change. The shape of the

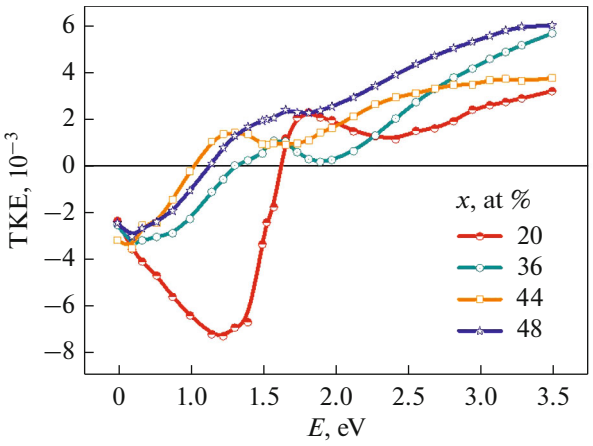

Fig. 7. The spectral dependences of the TKE of $CoFeB)_x(LiNbO_3)_{100-x}$ nanocomposites at room temperature; light incidence angle 69.5°.

spectrum is substantially different from the spectrum of $(CoFeB)_x(Al_2O_3)_{100-x}$ films with the same ferromagnetic material [12], but with a different dielectric. The shape of the spectrum of nanocomposites depends on many factors, such as the matrix material and the size and shape of magnetic nanoparticles; however, the material of ferromagnetic inclusions plays a dominant role [13]. Apparently, the composition of the granules depends not only on the composition of the target, but also on the technological conditions of film preparation.

CONCLUSIONS

Magneto-optical methods have shown that $(CoFeB)_x(LiNbO_3)_{100-x}$ nanocomposites with $x =$ 17 at % exhibit superparamagnetic behavior at temperatures above the blocking temperature 30 K.

The exchange coupling and the dipole–dipole interactions between grains begin to play an increasingly important role with an increase in the metal concentration, which leads to nonlinear field dependences of the TKE at room temperature without opening the hysteresis loop at $x \le 36$ at %. The anomalous field dependence of the MO signal at 36 at % proves the formation of a superferromagnetic state.

The long-range ferromagnetic order arises in the vicinity of 44 at %, i.e., at a metal concentration when the tunneling mechanism of conductivity still operates. Hence, the ferromagnetic percolation threshold is less than the transport percolation threshold.

FUNDING

This study was supported by the Russian Science Foundation (grant no. 22-29-00392) and was performed using the equipment purchased at the expense of Development Program of Moscow State University.

CONFLICT OF INTEREST

The authors declare that they have no conflicts of interest.

OPEN ACCESS

REFERENCES

1. V. V. Rylkov, A. V. Emelyanov, S. N. Nikolaev, K. E. Nikiruy, A. V. Sitnikov, E. A. Fadeev, V. A. Demin, A. B. Granovsky, "Transport properties of magnetic nanogranular composites with dispersed ions in an insulating matrix," J. Exp. Theor. Phys. **131**, 160–176 (2020). https://doi.org/10.1134/S1063776120070109
2. M. N. Martyshov, A. V. Emelyanov, V. A. Demin, K. E. Nikiruy, A. A. Minnekhanov, S. N. Nikolaev, A. N. Taldenkov, A. V. Ovcharov, M. Yu. Presnyakov, A. V. Sitnikov, A. L. Vasiliev, P. A. Forsh, A. B. Granovsky, P. K. Kashkarov, M. V. Kovalchuk, and V. V. Rylkov, "Multifilamentary character of anticorrelated capacitive and resistive switching in memristive structures based on $(CoFeB)_x(LiNbO_3)_{100-x}$ nanocomposite," Phys. Rev. Appl **14**, 034016 (2020). https://doi.org/10.1103/PhysRevApplied.14.034016
3. S. Bedanta and W. Kleemann, "Supermagnetism," J. Phys. D: Appl. Phys. **42**, 013001 (2008). https://doi.org/10.1088/0022-3727/42/1/013001
4. I. S. Beloborodov, A. V. Lopatin, V. M. Vinokur, and K. B. Efetov, "Granular electronic systems," Rev. Mod. Phys. **79**, 469 (2007). https://doi.org/10.1103/RevModPhys.79.469
5. V. V. Rylkov, S. N. Nikolaev, V. A. Demin, A. V. Emel'yanov, A. V. Sitnikov, K. E. Nikirui, V. A. Levanov, M. Yu. Presnyakov, A. N. Taldenkov, A. L. Vasil'ev, K. Yu. Chernoglazov, A. S. Vedeneev, Yu. E. Kalinin, A. B. Granovskii, V. V. Tugushev, and A. S. Bugaev, "Transportnye, magnitnye i memristivnye svoistva nanogranulirovannogo kompozita $(CoFeB)_x(LiNbO_y)_{100-x}$," J. Exp. Theor. Phys. **126**, 353–367 (2018). https://doi.org/10.1134/S1063776118020152
6. V. V. Rylkov, A. B. Drovosekov, A. N. Taldenkov, S. N. Nikolaev, O. G. Udalov, A. V. Emelyanov, A. V. Sitnikov, K. Yu. Chernoglazov, V. A. Demin, O. A. Novodvorskii, A. S. Vedeneev, and A. S. Bugaev, "Unusual behavior of the coercive field in a

$(CoFeB)_x(LiNbO_y)_{100-x}$ nanocomposite with a high content of magnetic ions in an insulating matrix," J. Exp. Theor. Phys. **128**, 115–124 (2019). https://doi.org/10.1134/S1063776119010163

7. S. N. Nikolaev, A. V. Emelyanov, R. G. Chumakov, V. V. Rylkov, A. V. Sitnikov, M. Yu. Presnyakov, E. V. Kukueva, and V. A. Demin, "The properties of memristive structures based on $(Co_{40}Fe_{40}B_{20})_x(LiNbO_3)_{100-x}$ nanocomposites synthesized on SiO2/Si substrates," Tech. Phys. **65**, 243–249 (2020). https://doi.org/10.1134/S1063784220020188

8. K. E. Nikiruy, A. V. Emelyanov, A. N. Matsukatova, E. V. Kukueva, A. L. Vasiliev, A. V. Sitnikov, V. A. Demin, and V. V. Rylkov, "Percolation effect impact on resistive switching of structures based on nanocomposite $(Co_{40}Fe_{40}B_{20})_x(LiNbO_3)_{100-x}$," Phys. Solid State **64**, 1665–1669 (2022). https://doi.org/10.21883/PSS.2022.11.54188.410

9. V. V. Rylkov, A. V. Sitnikov, S. N. Nikolaev, V. A. Demin, A. N. Taldenkov, M. Yu. Presnyakov, A. V. Emelyanov, A. L. Vasiliev, Yu. E. Kalinin, A. S. Bugaev, V. V. Tugushev, and A. B. Granovsky, "Properties of granular $(CoFeB)_x(Al_2O_3)_{100-x}$ and $(CoFeB)_x(LiNbO_y)_{100-x}$ nanocomposites: Manifestation of superferromagnetic ordering effects," J. Magn. Magn. Mater. **459**, 197–201 (2018). https://doi.org/10.1016/j.jmmm.2017.11.022

10. Magneto-optical Kerr microscope & magnetometer. http://evicomagnetics.com/productss/magneto-optical-kerr-microscope-magnetometer.

11. G. Traeger, L. Wenzel, and A. Hubert, "Computer experiments on the information depth and the figure of merit in magnetooptics," Phys. Status Solidi A **131**, 201–227 (1992). https://doi.org/10.1002/pssa.2211310131

12. E. A. Gan'shina, A. B. Granovsky, A. V. Sitnikov, E. Lahderanta, and V. V. Rylkov, "Magneto-optical spectroscopy of $(CoFeB)_x$–$(Al–O)_{100-x}$ nanocomposites: Evidence of superferromagnetism," IEEE Magn. Lett. **11**, 2500504 (2020). https://doi.org/10.1109/LMAG.2019.2963874

13. E. A. Gan'shina, M. V. Vashuk, A. N. Vinogradov, A. B. Granovskii, V. S. Gushchin, P. N. Shcherbak, Yu. P. Kalinin, A. V. Sitnikov, Ch.-O. Kim, and Ch. G. Kim, "Evolution of the optical and magnetooptical properties of amorphous metal-insulator nanocomposites," J. Exp. Theor. Phys. **98**, 1027–1036 (2004). https://doi.org/10.1134/1.1767571

Translated by O. Kadkin